Available online at www.sciencedirect.com
ScienceDirect
Fungal Genetics and Biology 44 (2007) 466–473
FUNGAL GENETICS AND BIOLOGY
www.elsevier.com/locate/yfgbi

Technological Advancement

Laser microdissection of fungal septa as visualised by scanning electron microscopy

Kenneth G.A. van Driel [a,*], Teun Boekhout [a], Han A.B. Wösten [b], Arie J. Verkleij [c], Wally H. Müller [c]

[a] *Centraalbureau voor Schimmelcultures (CBS), Royal Netherlands Academy of Arts and Sciences (KNAW), Utrecht, The Netherlands*
[b] *Molecular Microbiology, Institute of Biomembranes, Utrecht University, Utrecht, The Netherlands*
[c] *Cellular Architecture and Dynamics, Institute of Biomembranes, Utrecht University, Utrecht, The Netherlands*

Received 8 August 2006; accepted 24 October 2006
Available online 8 December 2006

Abstract

Laser microdissection has been proven a successful technique to isolate single cells or groups of cells from animal and plant tissue. Here, we demonstrate that laser microdissection is suitable to isolate subcellular parts of fungal hyphae. Dolipore septa of *Rhizoctonia solani* containing septal pore caps were cut by laser microdissection from sections of mycelium and collected by laser pressure catapulting. Subsequently, microdissected septa were visualised using a wheat germ agglutinin labelling of cell walls, septa and septal pore caps and scanning electron microscopy. The use of laser microdissection on fungal cells opens new ways to study subcellular fungal structures and the biochemical composition of hyphal cells.

Keywords: Laser microdissection; Laser pressure catapulting; PALM; Fungi; *Rhizoctonia solani*; Septum; Septal pore cap; Wheat germ agglutinin; Electron microscopy

1. Introduction

Laser microdissection has become a standard technique to select single cells or specific cell populations from animal or human tissue to study them separately from their heterogeneous environment. Recently, laser microdissection has also been used in plant research (Day et al., 2005; Nelson et al., 2006). Several laser microdissection techniques have been developed (Pinzani et al., 2006; Day et al., 2005), of which three systems are mainly used. First, the PixCell system (Arcturus Bioscience, Inc., Mountain View, CA, USA, www.arctur.com) that uses a near infrared laser to capture the cells of interest by fusing them to a thermoplastic film (Emmert-Buck et al., 1996). Second, the AS LMD laser microscope (Leica Microsystems AG, Wetzlar, Germany, www.leica-microsystems.com), which is a non-contact method that uses an UV laser of 337 nm wavelength to dissect cells, which then fall by gravity into a tube cap placed underneath the section (De Souza et al., 2004). Third, the PALM MicroBeam system (P.A.L.M. Microlaser Technologies AG, Bernried, Germany, www.palm-mikrolaser.com) that uses a pulsed UV-A laser of 337 nm wavelength to microdissect the cells of interest. This is combined with non-contact transfer by laser pressure catapulting (LPC), by which the force of a focused laser beam is used to overcome the gravity and to transfer the dissected tissue sample upwards into the cap of a sample tube placed above the section (Schütze and Lahr, 1999; Westphal et al., 2002).

Once the cells of interest are dissected and collected, their protein and genetic profile can be analysed by several down-stream applications. DNA and RNA extracted from the laser microdissected tissue can be subjected for instance to PCR (Wong et al., 2000), RT-PCR (Fend et al., 1999; Mojsilovic-Petrovic et al., 2004; Shimamura et al., 2004; Wang et al., 2004), real-time quantitative RT-PCR

* Corresponding author. Fax: +31 30 2512097.
E-mail address: vandriel@cbs.knaw.nl (K.G.A. van Driel).

1087-1845/$ - see front matter © 2006 Elsevier Inc. All rights reserved.
doi:10.1016/j.fgb.2006.10.006

(Wong et al., 2000), or gene expression studies (Scheidl et al., 2002; Burbach et al., 2003; Fuller et al., 2003; Mohr et al., 2004). RNA isolated from laser microdissected samples is of high quality and low copy number mRNA can be isolated (Mikulowska-Mennis et al., 2002). Proteins from laser microdissected tissue can be analysed for example by 2D-gel electrophoresis (Banks et al., 1999; Ornstein et al., 2000; Craven and Banks, 2001, 2002; Moulédos et al., 2003; De Souza et al., 2004), peptide mass fingerprinting (Craven et al., 2002), protein arrays (Grubb et al., 2003), immunoassays (Simone et al., 2000), and LC–MS/MS (Schad et al., 2005a). Compared to traditional isolation techniques, laser microdissection has no gross effects on protein profiles, antigenicity, and mass spectrometric profiles (Banks et al., 1999). Next to genetic and protein profiles it was demonstrated that cell-type specific metabolite profiles could be generated from laser microdissected plant tissue (Schad et al., 2005b).

Laser microdissection has also been applied in several studies in which bacterial, viral, and fungal infections were involved that were recognized either by morphological changes of the tissue (Ryan et al., 2002; Yazdi et al., 2004), or by visualization by fluorescence *in situ* hybridisation (FISH) (Klitgaard et al., 2005) or by using a fluorescent fungal cell wall stain (Xue et al., 2005). In addition, laser microdissection can also be applied for isolation of subcellular structures. For instance, individual chloroplasts could be isolated from plant cells for single-organelle analysis (Meimberg et al., 2003), and metaphase chromosomes were isolated from plant and animal cells (Schermelleh et al., 1999; Hobza et al., 2004).

In the current study, we used the PALM MicroBeam system to isolate fungal septa from hyphae of the filamentous basidiomcyete *Rhizoctonia solani*, which has dolipore septa with perforate septal pore caps (SPCs) (Bracker and Butler, 1963; Müller et al., 1998, 2000). Though many ultrastructural details of the SPC and the dolipore septum of *R. solani* are available (Bracker and Butler, 1963; Lisker et al., 1975; Müller et al., 1998, 2000), nothing is known about the composition of the dolipore–SPC complex. Therefore, an appropriate isolation technique of the SPC–dolipore complex is needed to understand its biochemical composition and hence its role in basidiomycete fungi. Here, laser microdissection is used for the first time to isolate fungal structures, and therefore we focus on the visualization of the isolated and collected septa to confirm the isolation procedure. The microdissected and laser catapulted septa were visualised by scanning electron microscopy using a WGA–gold–Ag labelling.

2. Materials and methods

2.1. Strain and growth conditions

Rhizoctonia solani CBS 346.84 was grown on malt extract agar (Oxoid, Hampshire, UK) for 4 days at 25 °C between two perforated polycarbonate (PC) membranes with a diameter of 47 mm and a 0.6 μm pore size (Poretics, Osmonics Inc., Minnetonka, MN, USA).

2.2. Preparation of mycelium for laser microdissection in buffer

The upper PC membrane was removed from the sandwiched culture and the mycelium was fixed with a picric acid and formaldehyde containing fixative (PA/FA fixative: 1.5 parts saturated picric acid (PA), 2.5 parts 8% (w/v) formaldehyde (FA), 5.0 parts 200 mM sodium citrate buffer, pH 6.2, and 1.0 part distilled water) (Müller et al., 2002). After 30 min, the mycelium was transferred to fresh PA/FA fixative and incubated for another 30 min. Then, the sandwich culture was washed and stored in 1% formaldehyde in phosphate buffered saline (PBS) (137.0 mM NaCl, 2.7 mM KCl, 8.1 mM Na_2HPO_4, and 1.5 mM KH_2PO_4) at 4 °C. Before use, cultures were washed with PBS. Parts of about 10×5 mm were cut from the periphery of the colony, placed on a microscope glass, and kept in buffer to prevent desiccation of the mycelium.

2.3. Cryo-sectioning and Lowicryl HM20 embedded sections

Sandwiched cultures were fixed in PA/FA fixative as described above and embedded in 12% (w/v) gelatine in PBS. Cubes of about 1 mm^3 were cut, infused with 2.3 M sucrose, mounted on a cutting pin and frozen for cryo-sectioning according to Tokuyasu (1973). Cryo-sections of about 150 nm and 1 μm thick were cut with a glass knife using a Leica cryo-ultramicrotome (Leica Microsystems AG, Wetzlar, Germany). The cryo-sections were picked-up with 2.3 M sucrose using a Perfect Loop (Electron Microscopy Sciences (EMS), Hatfield, PA, USA) and transferred to a formvar film-coated 1×2 mm single slot nickel grid (L2 × 1, Veco grid, EMS). The grids with cryo-sections were floated on droplets of PBS, with the section-side down, to remove the sucrose. Subsequently, the sections were stained with 0.25% (w/v) toluidine blue, and 0.5% (v/v) acetic acid in distilled water for 10 min to enhance the visibility of the hyphal cells and the identification of the septa. Sections were washed three times with distilled water and embedded in a thin film of methylcellulose (Müller et al., 2002) to prevent drying of the cryo-sections. The grids with cryo-sections were placed on a microscope glass slide.

As an alternative to cryo-sectioning, *R. solani* mycelium was low-temperature embedded in lowicryl HM20. Parts of the sandwiched cultures were first cryo-fixed by high-pressure freezing (HPF) using a Leica EM HPF (Leica). The mycelium was subsequently freeze-substituted in 0.3% (w/v) uranyl acetate and 0.01% (v/v) glutaraldehyde in anhydrous methanol, and infiltrated and low-temperature embedded in lowicryl HM20 as described by Müller et al. (2002). After 48 h of polymerisation at −40 °C and 24 h of polymerisation at room temperature under UV light, 300 nm thick sections were cut with a Diatome diamond knife (Diatome, Hatfield, PA,

USA) using a Leica ULTRACUT E ultramicrotome (Leica) and labelled as described below.

2.4. WGA–gold–Ag labelling of cell walls and septa

Sections were labelled and washed while floating and were transferred with a Perfect Loop between droplets. HM20 sections were blocked for 30 min with 3% (w/v) BSA-c (Aurion, Wageningen, The Netherlands) in TBS buffer (10 mM Tris–HCl, 100 mM NaCl, pH 7.4). Sections were subsequently incubated for 60 min with wheat germ agglutinin (WGA) conjugated to 10 nm colloidal gold (Sigma–Aldrich, St. Louis, MO, USA), 1:50 diluted in 0.1% (w/v) BSA-c. Sections were washed with 0.1% (w/v) BSA-c in TBS followed by three washes with PBS and three washes with distilled water for 5 min each. Gold particles were silver enhanced (Aurion) during 30 min at room temperature, and washed subsequently with distilled water. WGA–gold–Ag labelled HM20 sections were picked-up with a single hole nickel grid with an aperture of 2 mm (GA2000-Ni, EMS) and placed up side down on a PEN-membrane covered microscope slide (Fig. 1). Excess of fluid was removed by placing a small piece of Whatman paper against the rim of the grid.

2.5. Laser microdissection and laser pressure catapulting

Laser microdissection and laser pressure catapulting were performed with the PALM MicroBeam system (P.A.L.M. Microlaser Technologies AG) equipped with an Axiovert 200 Zeiss inverted microscope (Carl Zeiss AG, Oberkochen, Germany) and a 3CCD colour camera (HV-D30, Hitachi Kokusai Electric Inc., Tokyo, Japan). We selected fungal septa on the computer screen with the PALM RoboSoftware (v2.2). Around the septum a circle was drawn along which the laser followed to cut the septum. The laser power and laser focus were adjusted until the cut was at its narrowest during microdissection. The following settings have been used with a 40× objective: PA/FA fixed mycelium was microdissected using a laser UV energy setting of 76 and a focus setting of 51 in the PALM Robosoftware. Cryo-sections were microdissected using UV energy settings between 73 and 75, and UV focus settings of 51–52 in the PALM Robosoftware. The microdissected material was catapulted into the cap of a sample tube placed above the section. Lowicryl HM20 sections on a PEN membrane-covered microscope glass slide were cut using a laser UV energy setting of 67 and a focus setting of 50 in the P.A.L.M. software. The diameter of the dissected specimen was between 14.7 and 19.5 μm. The microdissected material was catapulted with an UV energy setting of about 77 in the PALM Robosoftware and collected on a formvar film-coated single slot grid (L2 × 1, Veco grid, EMS). A schematic representation of the laser microdissection and laser catapulting procedure of lowicryl HM20 sections is shown in Fig. 2.

2.6. Electron microscopy

Sections of HPF-fixed, freeze-substituted, and HM20 embedded *R. solani* hyphae were labelled with WGA–gold–Ag and viewed with a TECNAI 10 (FEI Company,

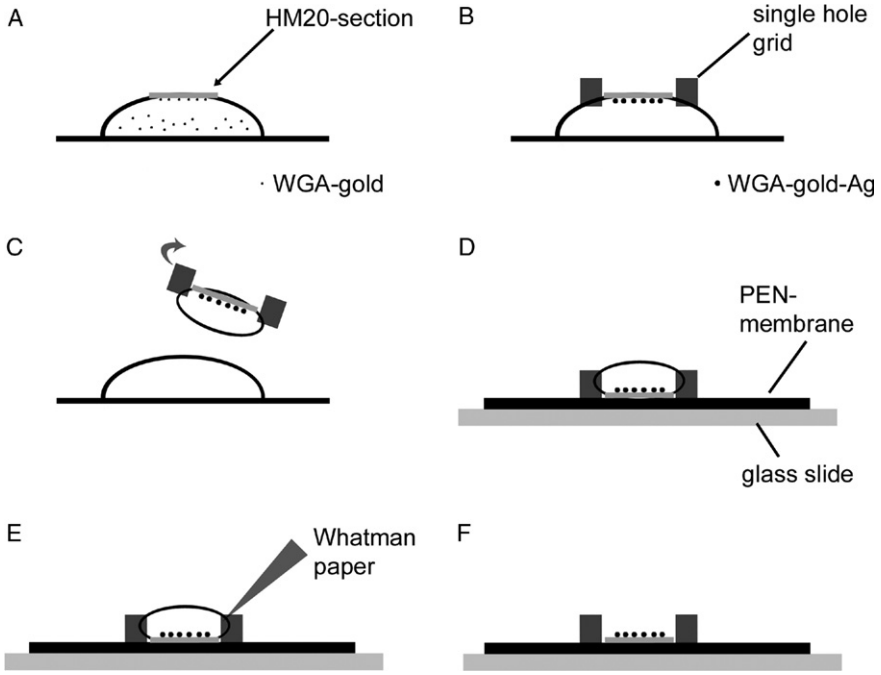

Fig. 1. Schematic representation of the preparation of labelled sections of *Rhizoctonia solani* hyphae embedded in HM20 placed on a PEN-membrane. Sections were labelled with WGA–gold and silver enhanced (A). A single hole grid (GA2000) was placed on the droplet in such a way that the grid enclosed the section (B). By picking up the grid, the section was taken from the droplet (C). The grid was subsequently placed up side down on a PEN-membrane covered microscope slide (D) and excess of fluid was removed with a piece of Whatman paper (E and F).

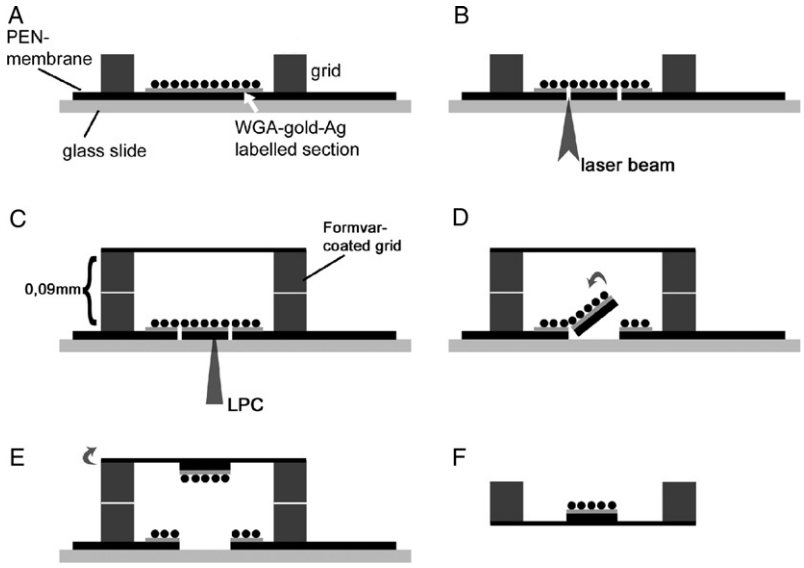

Fig. 2. Schematic representation of laser microdissection and laser pressure catapulting of septa of *Rhizoctonia solani* from WGA–gold–Ag labelled HM20 sections. A section was placed with a single hole grid on PEN-membrane (A) and microdissected with the laser (B). A formvar film-coated single slot grid (L2 × 1) was put on top of the single hole grid that enclosed the HM20 section and the microdissected region was catapulted upwards by LPC (C). During the transfer (D) the microdissected samples turned over and were collected at the formvar film-coated grid (E), which was analysed by electron microscopy (F).

Eindhoven, The Netherlands) transmission electron microscope at an acceleration voltage of 100 kV prior to laser microdissection. Microdissected and laser pressure catapulted HM20 embedded material was examined with a light microscope or an XL30 scanning field emission gun microscope (FEI Company). At low magnification, an acceleration voltage of 5.0 kV, spot size of 3.0, work distance of 5.0 mm and the SE detector were used (Fig. 7A and B). At high magnification, an acceleration voltage of 20.0 kV and the TLD detector were used with a spot size of 4.0 and a work distance of 5.1 mm (Fig. 7C) or a spot size of 3.0 and a work distance of 4.7 mm were used (Fig. 7D and E).

3. Results

3.1. Laser microdissection of fungal septa from mycelium in buffer

Picric acid and formaldehyde fixed mycelium of *R. solani* was placed on a microscope slide with adherent buffer. We did not use air-dried mycelium or critical point dried mycelium, because the septa could not be recognized anymore (result not shown). The septa were selected on the computer screen (Fig. 3A), microdissected with the laser (Fig. 3B and C), and released into the surrounding buffer (Fig. 3C). However, the released septa could not be collected in the cap of a sample tube by laser pressure catapulting (LPC), as was shown by light microscopy (data not shown). In addition, the LPC shot, used to transfer the microdissected samples upwards, affected a larger proportion of the mycelium than only the dissected septum, resulting in a dislocation of the surrounding hyphae (result not shown). Though the hyphae were successfully cut by the laser, the microdissected septa could not be collected from fluid by LPC.

3.2. Laser microdissection and laser pressure catapulting of fungal septa from cryo-sections

Transmission electron microscopy showed that dolipore septa with associated perforate septal pore caps were well

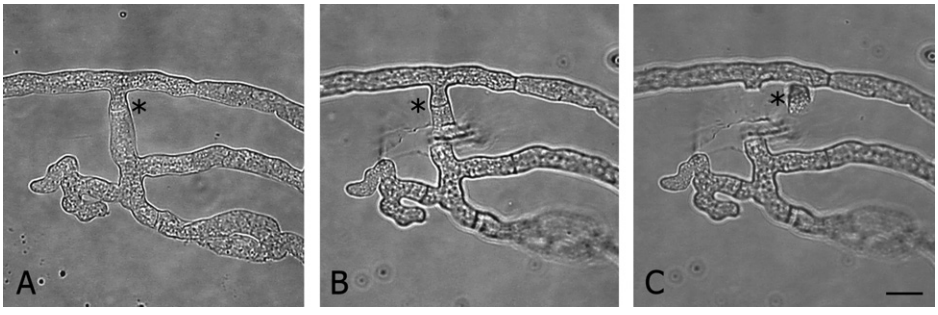

Fig. 3. Light microscopic images of picric acid and formaldehyde fixed *Rhizoctonia solani* hyphae in buffer before (A) and after (B and C) laser microdissection at either side of a septum indicated with an asterisk. Bar represents 10 μm.

preserved in picric acid and formaldehyde fixed *R. solani* mycelium (Fig. 4). Preceding laser microdissection, the cryo-sections were stained with toluidine blue to enhance contrast of the hyphal cells and the septa (Fig. 5A). The septa were laser microdissected around (Fig. 5B), and transferred upwards in the cap of a sample tube by LPC, thereby leaving small holes in the cryo-section (Fig. 5C). However, the collected material was wrinkled, therefore hampering examination by electron microscopy (data not shown). Thus, cryosections could be successfully microdissected and fungal septa could be collected by LPC, but the material cannot be examined by electron microscopy.

3.3. Laser microdissection and laser pressure catapulting of fungal septa from lowicryl HM20 embedded mycelium

Sections of HPF-fixed, freeze-substituted and lowicryl HM20 embedded *R. solani* mycelium were labelled with WGA–gold, and subsequently silver enhanced (Fig. 1). Cell walls, septa and septal pore caps were decorated with gold–Ag particles as visualized by transmission electron microscopy (TEM) (Fig. 6). The WGA–gold–Ag labelled sections were placed on a PEN-membrane covered microscope slide with the labelled side upwards (Fig. 2) and septal regions were selected on the computer screen. After laser microdissection, a formvar film-coated single slot grid was placed on top of the single hole grid that enclosed

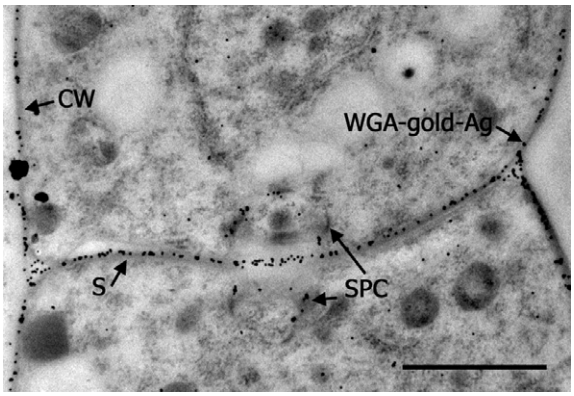

Fig. 6. Transmission electron micrograph of part of a HPF-fixed, freeze-substituted and HM20 embedded *Rhizoctonia solani* hypha that was labelled with WGA–gold and silver-enhanced. Cell walls, septum, and septal pore caps were decorated with WGA–gold–Ag. Bar represents 2 μm. CW, cell wall; S, septum; SPC, septal pore cap.

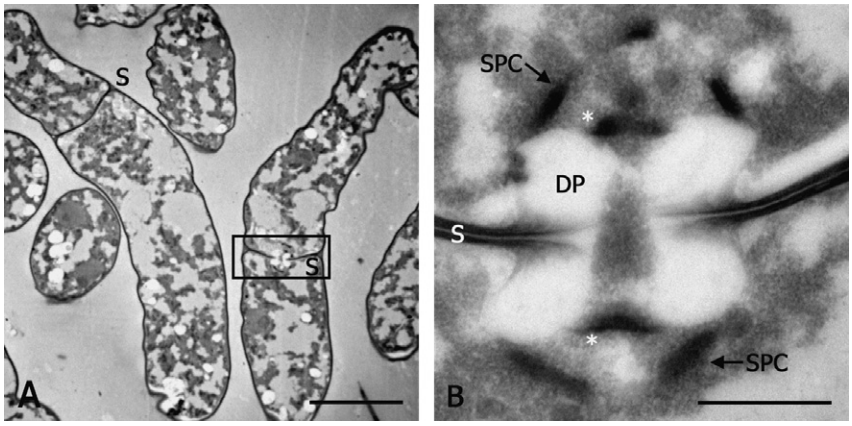

Fig. 4. Transmission electron micrograph of a 150 nm cryo-section of picric acid and formaldehyde fixed *Rhizoctonia solani* hyphae. (A) Overview of longitudinally sectioned hyphae. The box indicates the septum with the dolipore and associated septal pore caps. (B) Higher magnification of a part of the septum as shown in (A). Perforate SPCs cover the dolipore septum at both sides. Electron-dense plugging material (∗) is present at the orifice of the dolipore. Bar represents 10 μm (A) and 1 μm (B). S, septum; DP, dolipore; SPC, septal pore cap.

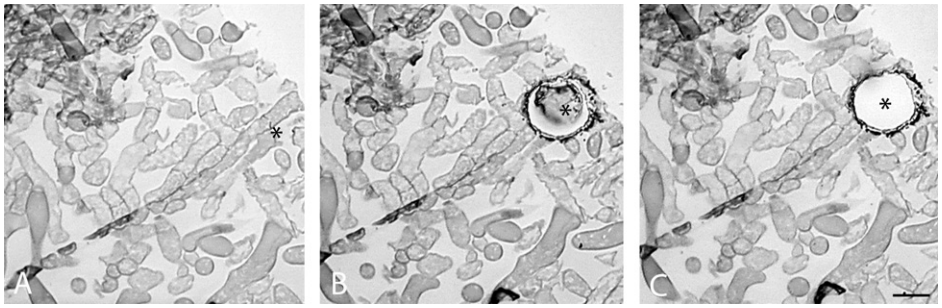

Fig. 5. Light microscopic images of 1 μm thick cryo-sections of *Rhizoctonia solani* mycelium stained with toluidine blue before (A) and after (B) laser microdissection. The septum of interest (∗) was microdissected along a predrawn circle (B) and subsequently laser pressure catapulted (C). Bar represents 10 μm.

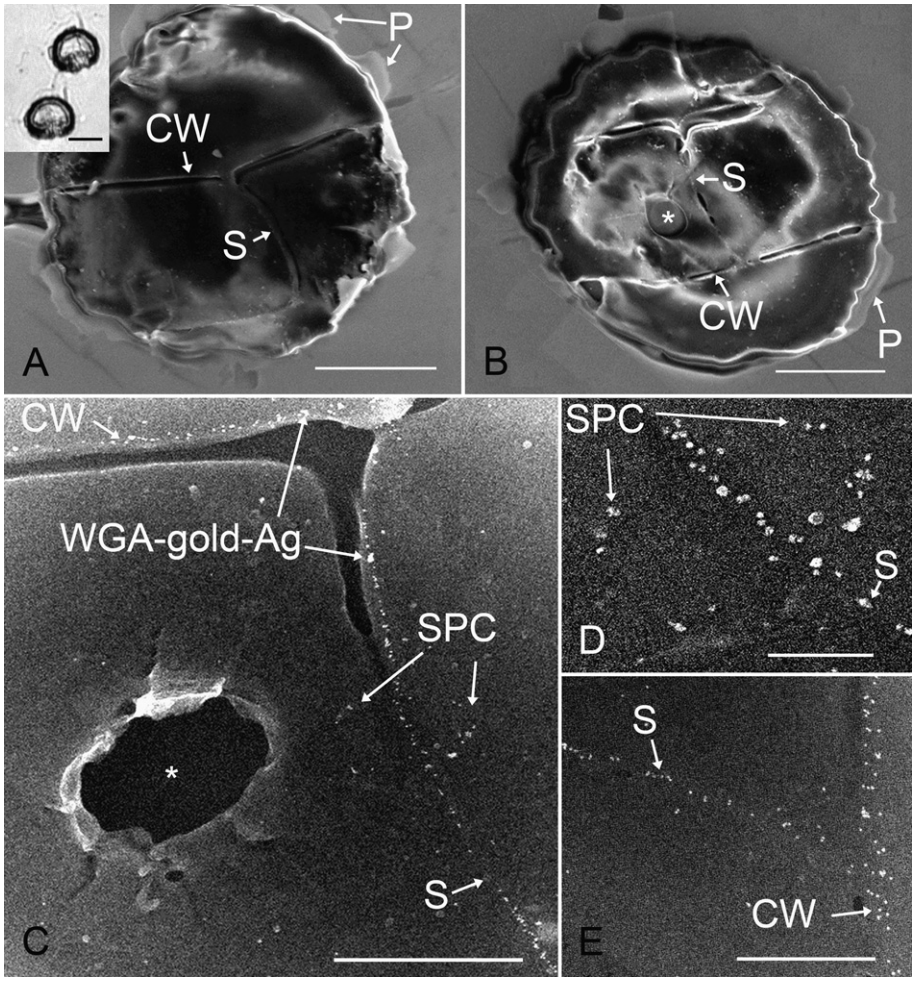

Fig. 7. Scanning electron micrographs of laser microdissected septa of *Rhizoctonia solani* that were WGA–gold–Ag labelled and collected by laser pressure catapulting (LPC) to a formvar film. (A) Low magnification of a microdissected stack that consisted of PEN-membrane and part of a HM20 embedded hypha with a septum. Inset shows light microscopic visualization of microdissected septa collected on a formvar film by LPC. (B) Low magnification of a laser microdissected stack, in which the LPC shot introduced a hole (∗) at the site where the LPC shot hit the microdissected stack to transfer it upwards. (C) High magnification of a microdissected septum showing the gold–Ag particles (arrows) that decorated the cell walls, septum and septal pore caps and a hole that was introduced by an LPC shot (∗). (D) Higher magnification of a part of the septum as shown in (C) with WGA–gold–Ag labelling of septum and both septal pore caps. (E) Higher magnification of a part of the septum showing WGA–gold–Ag labelling of cell wall and septum. Bar represents 5 μm (A and B), 10 μm (inset A), 2 μm (C), 0.5 μm (D), and 1μm (E). CW, cell wall; S, septum; SPC, septal pore cap; P, PEN-membrane.

the HM20 section (Fig. 2). Examination of the grids in the scanning electron microscope showed a thickness of about 0.045 mm each, thus resulting in a total transfer distance of about 0.09 mm between the sample and the formvar film. The microdissected material was transferred upwards by LPC, and collected at the formvar film as was observed by light microscopy (inset of Fig. 7A). The microdissected stack consisting of PEN-membrane and the microdissected septum in HM20, appeared electron impermeable in the TEM at 100 kV (result not shown), but could be examined by scanning electron microscopy (Fig. 7A and B). Furthermore, at the site where the LPC shot hit the microdissected stack to transfer it upwards (Fig. 7B and C), a hole was visible occasionally (Fig. 7B and C). Examination at high magnification showed WGA–gold–Ag labelling of the cell walls, septa, and septal pore caps at the surface of the microdissected HM20 section (Fig. 7C–E).

4. Discussion

Laser microdissection is a powerful tool to obtain pure samples of specific cells or subcellular structures and is more and more routinely used in animal and plant studies. Surprisingly, laser microdissection has not been used to study fungi or fungal subcellular structures. Although fungal cells are much smaller compared to animal or plant cells, they can be viewed with a light microscope, which is a prerequisite for laser microdissection. We report here the use of laser microdissection to cut fungal hyphae. Dolipore septa with associated septal pore caps were laser microdissected and collected by laser pressure catapulting (LPC) from hyphae of *R. solani* as was shown by scanning electron microscopy. The presented isolation method allows future biochemical analysis of the dolipore septum and septal pore caps, necessary for understanding its function in the fungal cell.

Fixation of the *R. solani* mycelium is necessary to prevent leakage of the cellular content from the hyphae during microdissection. Ethanol and formaldehyde fixations are often used in laser microdissection studies (Ahram et al., 2003). Precipitative fixatives (e.g., ethanol, acetone) are preferred above crosslinking fixatives (e.g., formaldehyde, glutaraldehyde), because the cross-linking effects reduces the amount of extractable DNA, RNA, and proteins (Day et al., 2005). However, ethanol fixation resulted in poor morphology of the septal region, and therefore a 2% formaldehyde-containing fixative was used instead. Low percentage formaldehyde fixations form reversible crosslinkings, and future DNA, RNA, and protein extractions of the microdissected hyphae will be possible (Baschong et al., 1983; Finke et al., 1993; Pinzani et al., 2006). Future studies have to determine the most optimal fixative that gives both a good histological detail of the tissue and good recovery of the biomolecules of interest (Nelson et al., 2006).

Though we were able to microdissect the septal area from fixed *R. solani* hyphae in buffer, we could not collect these selected parts by LPC. Probably, the LPC energy was not powerful enough to overcome the water surface tension of the buffer to catapult the septum out of the buffer. Furthermore, the LPC energy was transferred to a larger area than the selected point of catapulting and changed the position of the sample. To collect the microdissected material in buffer, optical tweezers should be used (reviewed by Grier, 2003), for example, the PALM MicroTweezers (P.A.L.M. Microlaser Technologies AG). When a laser microdissection microscope is not equipped with optical tweezers, sectioned tissue is needed to overcome the collection difficulties. For this reason, we used cryo-ultramicrotomy or a combination of high pressure freezing, freeze substitution, and low temperature embedding.

Cryo-sectioning according to Tokuyasu (1973) is a technique compatible with mild fixation without other denaturing steps involved, like dehydration with organic solvents or embedding in resins. This makes cryo-sectioned tissue useful for future extraction and analysis of DNA, RNA, and proteins. Although laser microdissection of the cryo-sections of *R. solani* hyphae was successful, we could not verify whether fungal septa were collected after laser pressure catapulting. During its transport to the collection cap by the LPC shot, the microdissected material became wrinkled, hence, impossible to examine by light or electron microscopy. To examine the microdissected septa by electron microscopy, to confirm the isolation procedure, we used sections of lowicryl HM20 embedded *R. solani* mycelium that were labelled with WGA–gold–Ag, a lectin that binds the *N*-acetylglucosamine residues in cell walls and septa (Benhamou et al., 1993). Furthermore, the sections were placed on a PEN-membrane covered slide to give them extra support during the transfer. After laser microdissection and transfer of the septa by LPC to a formvar film-coated single slot grid (Fig. 2), we observed by scanning electron microscopy that most microdissected septa did not transfer vertically, but instead, turned over during the transfer (Fig. 2). WGA–gold–Ag labelling of the cell walls, septum, and septal pore caps verified microdissection and transfer by laser pressure catapulting of fungal septa.

Here, we show the potential of laser microdissection as an isolation tool in fungal cell biological research. Specific hyphae or hyphal cells could be isolated from a mycelium in order to analyze their biomolecules. Alternatively, parts of hyphae such as tips or subapical regions or organelles such as individual nuclei can be isolated and studied individually.

Acknowledgments

We express our thanks to Dr. Elly Hol (Netherlands Institute for Brain Research) for technical advice and using the PALM Microbeam system (Figures 3 and 5). We also like to thank DSM Food Specialties (Delft, The Netherlands) and SenterNovem (The Netherlands) for using their PALM Microbeam system (Figure 7). This work was financially supported by the Odo van Vloten foundation.

References

Ahram, M., Flaig, M.J., Gillespie, J.W., Duray, P.H., Linehan, W.M., Ornstein, D.K., Niu, S., Zhao, Y., Petricoin, E.F., Emmert-Buck, M.R., 2003. Evaluation of ethanol-fixed, paraffin-embedded tissues for proteomic applications. Proteomics 3, 413–421.

Banks, R.E., Dunn, M.J., Forbes, M.A., Stanley, A., Pappin, D., Naven, T., Gough, M., Harnden, P., Selby, P.J., 1999. The potential use of laser capture microdissection to selectively obtain distinct populations of cells for proteomic analysis—preliminary findings. Electrophoresis 20, 689–700.

Baschong, W., Baschong-Prescianotto, C., Kellenberger, E., 1983. Reversible fixation for the study of morphology and macromolecular composition of fragile biological structures. Eur. J. Cell Biol. 32, 1–6.

Benhamou, N., Broglie, K., Broglie, R., Chet, I., 1993. Antifungal effect of bean chitinase on *Rhizoctonia solani*: ultrastructural changes and cytochemical aspects of chitin breakdown. Can. J. Microbiol. 39, 318–328.

Bracker, C.E., Butler, E.E., 1963. The ultrastructure and development of septa in hyphae of *Rhizoctonia solani*. Mycologia 55, 35–58.

Burbach, G.J., Dehn, D., Del Turco, D., Deller, T., 2003. Quantification of layer-specific gene expression in the hippocampus: effective use of laser microdissection in combination with quantitative RT-PCR. J. Neurosci. Meth. 131, 83–91.

Craven, R.A., Banks, R.E., 2001. Laser capture microdissection and proteomics: possibilities and limitation. Proteomics 1, 1200–1204.

Craven, R.A., Totty, N., Harnden, P., Selby, P.J., Banks, R.E., 2002. Laser capture microdissection and two-dimensional polyacrylamide gel electrophoresis: evaluation of tissue preparation and sample limitations. Am. J. Pathol. 160, 815–822.

Day, R.C., Grossniklaus, U., Macknight, R.C., 2005. Be more specific! Laser-assisted microdissection of plant cells. Trends Plant Sci. 10, 397–406.

Emmert-Buck, M.R., Bonner, R.F., Smith, P.D., Chuaqui, R.F., Zhuang, Z., Goldstein, S.R., Weiss, R.A., Liotta, L.A., 1996. Laser capture microdissection. Science 274, 998–1001.

Fend, F., Emmert-Buck, M.R., Chuaqui, R., Cole, K., Lee, J., Liotta, L.A., Raffeld, M., 1999. Immuno-LCM: laser capture microdissection of

immunostained frozen sections for mRNA analysis. Am. J. pathol. 154, 61–66.
Finke, J., Fritzen, Ternes, P., Lange, W., Dölken, G., 1993. An improved strategy and a useful housekeeping gene for RNA analysis from formalin-fixed paraffine-embedded tissues by PCR. Biotechniques 14, 448–453.
Fuller, A.P., Palmer-Toy, D., Erlander, M.G., Sgroi, D.C., 2003. Laser capture microdissection and advanced molecular analysis of human breast cancer. J. Mammary Gland Biol. Neoplasia 8, 335–345.
Grier, D.G., 2003. A revolution in optical manipulation. Nature 424, 810–816.
Grubb, R.L., Calvert, V.S., Wulkuhle, J.D., Paweletz, C.P., Linehan, W.M., Phillips, J.L., Chuaqui, R., Valasco, A., Gillespie, J., Emmert-Buck, M., Liotta, L.A., Petricoin, E.F., 2003. Signal pathway profiling of prostate cancer using reverse phase protein arrays. Proteomics 3, 2142–2146.
Hobza, R., Lengerova, M., Cernohorska, H., Rubes, J., Vyskot, B., 2004. FAST-FISH with laser beam microdissected DOP-PCR probe distinguishes the sex chromosomes of *Silene latifolia*. Chromosome Res. 12, 245–250.
Klitgaard, K., Molbak, L., Jensen, T.K., Lindboe, C.F., Boye, M., 2005. Laser capture microdissection of bacterial cells targeted by fluorescence in situ hybridization. Biotechniques 39, 864–868.
Lisker, N., Katan, J., Henis, Y., 1975. Scanning electron microscopy of the septal pore apparatus of *Rhizoctonia solani*. Can. J. Bot. 53, 1801–1804.
Meimberg, H., Thalhammer, S., Brachmann, A., Müller, B., Eichacker, L.A., Heckl, W.M., Heubl, G., 2003. Selection of chloroplasts by laser microbeam microdissection for single-chloroplast PCR. Biotechniques 34, 1238–1243.
Mikulowska-Mennis, A., Taylor, T.B., Vishnu, P., Michie, S.A., Raja, R., Horner, N., Kunitake, S.T., 2002. High-quality RNA from cells isolated by laser capture microdissection. Biotechniques 33, 176–179.
Mohr, S., Bottin, M.-C., Lannes, B., Neuville, A., Bellocq, J.-P., Keith, G., Rihn, B.H., 2004. Microdissection, mRNA amplification and microarray: a study of pleural mesothelial and malignant mesothelioma cells. Biochimie 86, 13–19.
Mojsilovic-Petrovic, J., Nesic, M., Pen, A., Zhang, W., Stanimirovic, D., 2004. Development of rapid staining protocols for laser-capture microdissection of brain vessels from human and rat coupled to gene expression analyses. J. Neurosci. Meth. 133, 39–48.
Moulédos, L., Hunt, S., Harcourt, R., Harry, J.L., Williams, K.L., Gutstein, H.B., 2003. Proteomic analysis of immunostained, laser-capture microdissected brain samples. Electrophoresis 24, 296–302.
Müller, W.H., Stalpers, J.A., van Aelst, A.C., Krift, T.P., van der Boekhout, T., 1998. Field emission gun-scanning electron microscopy of septal pore caps of selected species in the *Rhizoctonia* s.l. complex. Mycologia 90, 170–179.
Müller, W.H., Koster, A.J., Humbel, B.M., Ziese, U., Verkleij, A.J., van Aelst, A.C., Krift, T.P., Montijn, R.C., Boekhout, T., 2000. Automated electron tomography of the septal pore cap in *Rhizoctonia solani*. J. Struct. Biol. 131, 10–18.
Müller, W.H., Thomassen, Y.E., Sagt, C.M.J., Humbel, B.M., 2002. Immuno-electron microscopy in yeast cell research. Rec. Res. Dev. Mol. Microbiol. 1, 1–25.
Nelson, T., Tausta, S.L., Gandotra, N., Liu, T., 2006. Laser microdissection of plant tissue: what you see is what you get. Annu. Rev. Plant Biol. 57, 181–201.
Ornstein, D.K., Gillespie, J.W., Paweletz, C.P., Duray, P.H., Herring, J., Vocke, C.D., Topalian, S.L., Bostwick, D.G., Linehan, W.M., Petricoin 3rd, E.F., Emmert-Buck, M.R., 2000. Proteomic analysis of laser capture microdissected human prostate cancer and in vitro prostate cell lines. Electrophoresis 21, 2235–2242.
Pinzani, P., Orlando, C., Pazzagli, M., 2006. Laser-assisted microdissection for real-time PCR sample preparation. Mol. Med. 27, 140–159.
Ryan, P., Bennett, M.W., Aarons, S., Lee, G., Collins, J.K., O'Sullivan, G.C., O'connell, J., Shanahan, F., 2002. PCR detection of *Mycobacterium paratuberculosis* in Crohn's disease granulomas isolated by laser capture microdissection. Gut 51, 665–670.
Schad, M., Lipton, M.S., Giavalisco, P., Smith, R.D., Kehr, J., 2005a. Evaluation of two-dimensional electrophoresis and liquid chromatography-tandem mass spectrometry for tissue-specific protein profiling of laser-microdissected plant samples. Electrophoresis 26, 2729–2738.
Schad, M., Mungur, R., Fiehn, O., Kehr, J., 2005b. Metabolic profiling of laser microdissected vascular bundles of *Arabidopsis thaliana*. Plant Meth. 1, 1–10.
Schermelleh, L., Thalhammer, S., Heckl, W., Pösl, H., Cremer, T., Schütze, K., Cremer, M., 1999. Laser microdissection and laser pressure catapulting for the generation of chromosome-specific paint probes. Biotechniques 27, 362–367.
Schütze, K., Lahr, G., 1999. Use of laser technology for microdissection and isolation. Am. Biotechnol. Lab., 24–30.
Scheidl, S.J., Nilsson, S., Kalén, M., Hellström, M., Takemoto, M., Håkansson, J., Lindahl, P., 2002. mRNA expression profiling of laser microbeam microdissected cells from slender embryonic structures. Am. J. Pathol. 160, 801–813.
Shimamura, M., Garcia, J.M., Prough, D.S., Hellmich, H.L., 2004. Laser capture microdissection and analysis of amplified antisense RNA from distinct cell populations of the young and aged rat brain: effect of traumatic brain injury on hippocampal gene expression. Mol. Brain. Res. 122, 47–61.
Simone, N.L., Remaley, A.T., Charboneau, L., Petricoin, E.F., Glickman, J.W., Emmert-Buck, M.R., Fleisher, T.A., Liotta, L.A., 2000. Sensitive immunoassay of tissue cell proteins procured by laser capture microscopy. Am. J. Path. 156, 445–452.
De Souza, A.I., McGregor, E., Dunn, M.J., Rose, M.L., 2004. Preparation of human heart for laser microdissection and proteomics. Proteomics 4, 578–586.
Tokuyasu, K.T., 1973. A technique for ultracryotomy of cell suspensions and tissues. J. Cell Biol. 57, 551–565.
Wang, X., Nakamura, M., Mori, I., Takeda, K., Nakamura, Y., Utsunomiya, H., Yoshimura, G., Sakurai, T., Kakudo, K., 2004. Calcitonin receptor gene and breast cancer: quantitative analysis with laser capture microdissection. Breast Cancer Res. Treatm. 83, 109–117.
Westphal, G., Burgemeister, R., Friedemann, G., Wellmann, A., Wernert, N., Wollscheid, V., Becker, B., Vogt, T., Knuchel, R., Stolz, W., Schutze, K., 2002. Noncontact laser catapulting: a basic procedure for functional genomics and proteomics. Methods Enzymol. 356, 80–99.
Wong, M.H., Saam, J.R., Stappenbeck, T.S., Rexer, C.H., Gordon, J.I., 2000. Genetic mosaic analysis based on Cre recombinase and navigated laser capture microdissection. Proc. Natl. Acad. Sci. USA 97, 12601–12606.
Xue, J., Hung, C.-Y., Yu, J.-J., Cole, G.T., 2005. Immune response of vaccinated and non-vaccinated mice to *Coccidioides posadasii* infection. Vaccine 23, 3535–3544.
Yazdi, A.S., Puchta, U., Flaig, M.J., Sander, C.A., 2004. Laser-capture microdissection: applications in routine molecular dermatopathology. J. Cutan. Pathol. 31, 465–470.